Inorganic Chemistry

Article

pubs.acs.org/IC

Trends in the Electronic Structure of Extended Gold Compounds: Implications for Use of Gold in Heterogeneous Catalysis

Mao-Sheng Miao,[†,‡] Joshua A. Kurzman,[†] Nisha Mammen,[§] Shobhana Narasimhan,[§] and Ram Seshadri*[,†]

[†]Department of Chemistry and Biochemistry, Materials Department, and Materials Research Laboratory, University of California, Santa Barbara, California 93106, United States

[‡]Beijing Computational Science Research Center, Beijing, 100089, P. R. China

[§]Theoretical Sciences Unit, Jawaharlal Nehru Centre for Advanced Scientific Research, Bangalore 560064 India

ABSTRACT: First-principles electronic structure calculations are presented on a variety of Au compounds and species—encompassing a wide range of formal oxidation states, coordination geometries, and chemical environments—in order to understand the potentially systematic behavior in the nature and energetics of d states that are implicated in catalytic activity. In particular, we monitor the position of the d-band center, which has been suggested to signal catalytic activity for reactions such as CO oxidation. We find a surprising absence of any kind of correlation between the formal oxidation state of Au and the position of the d-band center. Instead, we find that the center of the d band displays a nearly linear dependence on the degree of its filling, and this is a general relationship for Au irrespective of the chemistry or geometry of the particular Au compound. Across the compounds examined we find that even small calculated changes in the d-band filling result in a relatively large effect on the position of the d-band center. The results presented here have some important implications for the question of the catalytic activity of Au and indicate that the formal oxidation state is not a determining factor.

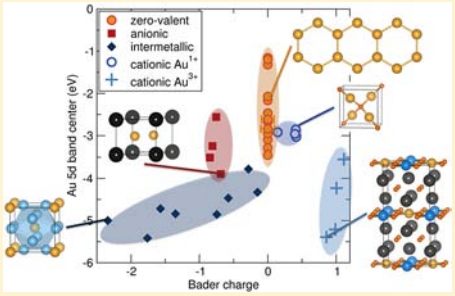

INTRODUCTION

Gold, that most noble of metals, is perforce not catalytically active in the bulk. However, even in the early 1800s Dulong and Thénard employed gold to catalyze the reaction of hydrogen and oxygen[1] and the decomposition of ammonia.[2] The new era in catalysis by gold, jump started by Haruta,[3] has given rise to extensive ongoing research, with a key goal being to address the origin of the catalytic activity of nanoscopic gold and the nature of the active species. Many different factors have been suggested to be responsible for the exceptional change in chemical behavior that occurs in reducing the particle size of gold to the nanoscale, such as quantum size effects,[4] onset of the metal-to-insulator transition,[5] interactions at metal−support interfaces,[6] and participation of charged gold species.[7] The possible role of oxidized or reduced gold species and the oxidation state of such species has been a widely debated topic: for reactions such as the oxidation of CO[7−16] and water−gas shift[17−21] there remains little consensus on whether cationic gold, anionic gold, metallic gold, or combinations thereof is responsible for the observed activity.

Certainly there is compelling evidence for participation of undercoordinated atoms on the surfaces of clusters and nanoparticles,[22−27] a concept with historic roots dating back to the nonuniform catalyst surface envisioned by Taylor.[28] The appreciable activity of unsupported nanoporous gold for the oxidation of CO[29] supports the notion that the presence of charged species is not a requisite for gold to behave catalytically.

The nobleness of bulk gold is attributed to relatively low-lying 5d states and, consequently, the filling of adsorbate−metal d antibonding states when molecules interact with its surface, thereby preventing adsorption.[30] Nanoscopic gold contains a large proportion of undercoordinated surface atoms, and for these atoms the center of the d band is believed to be nearer to the Fermi energy (E_F).[23,24,27] This can push the antibonding adsorbate states above E_F and stabilize chemisorption. Nørskov and co-workers developed an extensive body of work relating how the energy of transition metal d states influences adsorbate−substrate interactions, commonly known as the d-band model.[31−35] The d-band model provides a qualitative and quantitative framework in which to evaluate and predict trends in the catalytic activity of transition metal and alloy surfaces. In general, the closer the d states are to the Fermi energy, the stronger an adsorbate will bind to a surface since the antibonding states of the adsorbate will be less filled. Nørskov and co-workers have shown that because activation energies are related to the stability of intermediates, there is a universal (reactant independent) correlation between adsorption energies and catalytic activity.[36] Thus, adsorption behavior and therefore catalytic activity can be tuned by manipulating the position of transition metal d bands with respect to the Fermi energy. The often encountered volcano relations are easily understood in this context: a catalyst must not bind an adsorbate too strongly or the surface will become poisoned; on

Received: February 4, 2012
Published: July 5, 2012

   dx.doi.org/10.1021/ic3002674 | *Inorg. Chem.* 2012, 51, 7569−7578

the other hand, if the adsorbate does not bind strongly enough then the low surface coverages that result preclude high turnover rates. Numerous successes in the understanding and design of catalytic materials have been demonstrated based on these and related principles.[37−39] The d-band energy is a somewhat coarse-grained descriptor for predicting the reactivity of transition metal surfaces. More fine-grained descriptors have been developed in the context of catalysis by Au nanoparticles and clusters, for example, in the use of frontier molecular orbital theory, by Metiu and co-workers.[40,41]

As a strategy for addressing questions surrounding the possible catalytic role of ionic gold and platinum group species, we looked to well-defined model compounds and recently reported a comparison of two highly stable oxides containing square planar and isoelectronic Au^{3+} and Pd^{2+}, La_4LiAuO_8 and La_2BaPdO_5.[42] Given that Pd^{2+} and Pt^{2+} in the solid state are well known to catalyze a variety of reactions,[43] a natural question is whether Au^{3+} can behave similarly. We determined that La_4LiAuO_8 is a very poor catalyst for oxidation of CO to CO_2, in contrast to La_2BaPdO_5, which is quite a good catalyst for this reaction, despite being tested as a low surface area bulk powder. Electronic structure calculations reveal distinct differences in the average energy of the Pd 4d and Au 5d states—the Au d states are held deep below the Fermi energy with the centroid positioned at approximately −5.0 eV. The Pd d states of La_2BaPdO_5, on the other hand, are only about 2.5 eV below E_F. In the context of the d-band model, the distinct behaviors of these isoelectronic model compounds can be interpreted in terms of the differing abilities to interact with adsorbates: the d states of La_4LiAuO_8 are not accessible, while the d states of La_2BaPdO_5 are. Thus, we were led to the following question: If the d states of cationic Au^{3+} are too stabilized to be of interest for catalysis, where are the d states located in compounds containing formally or partially anionic gold?

Although a number of compounds of Au^- are known,[44] none of them are sufficiently stable to warrant catalytic testing and many are air sensitive; for example, dealloying of alkali−Au films exposed to O_2 has been found to occur near room temperature.[45,46] $Au^{\delta-}$ species, however, which are encountered in polar intermetallics of Au with the early transition metals, are comparatively quite stable. As we began to study ordered gold alloys, however, similarities in the electronic structure of gold compounds containing Au in vastly different formal oxidation states quickly became apparent. It became clear, as we shall demonstrate here, that the formal oxidation state of Au was uninformative about the electronic structural features that dictate catalytic activity.

Here we present first-principles bulk electronic structure calculations on a variety of Au compounds and species, encompassing a wide spectrum of formal oxidation states, coordination geometries, and chemical environments, and demonstrate that the center of the d band is linearly dependent on the degree of d-band filling. This is a general relationship for Au irrespective of its surroundings. Although changes in the d-band filling are small, the population of the d shell has a significant effect on the energy of the Au d states. By probing the electronic structure of well-defined gold compounds, this work emphasizes the somewhat unique electronic structural features encountered in undercoordinated gold, characterized by nanoparticles.

METHODS: COMPUTATIONAL DETAILS

The electronic structures of various Au, and Ag compounds were studied by the density functional theory (DFT) method. Calculations were performed using the Vienna ab initio Simulation Package (VASP),[47,48] employing the projector-augmented wave (PAW) method[49,50] and the Perdew−Burke−Ernzerhof (PBE) generalized gradient approximation (GGA) of exchange correlation.[51] The GGA +*U* method was also separately employed in order to take into account the potential for orbital-dependent Coulomb and exchange interactions. Geometric parameters including the lattice constants and internal atomic coordinates were optimized in all of the calculations, initialized with structural parameters listed in the Inorganic Crystal Structures Database (ICSD).[52] In order to ensure convergence of the total energy, forces, and stresses, a high cutoff energy of 550 eV was used in all calculations. The *k*-mesh grid employed varied across the different compounds but was in all cases tested for convergence. All calculations were performed at the scalar relativistic level, which is important for gold. Spin−orbit coupling (SOC) was not taken into account. SOC is believed to be important in low-dimensional gold species, such as gold chains.[53] However, from the data displayed in ref 54, the d-band center in a number of neutral gold structures of varying dimensionality is relatively unaffected by the presence or absence of SOC.

The charges on Au were determined by the Bader method with the aid of the Bader analysis program,[55] based on the atoms in molecules (AIM) theory.[56] The d-band center was computed as the first moment of the d-band projected density of states, referenced to the Fermi energy. Filling of the d states was calculated by integrating the d-projected density of states up to the Fermi energy or to the top of the valence band in the case of insulating compounds.

In view of the fact that the d-projected densities of state (DOS) is calculated within a finite sphere enclosing Au or Ag, not all of the charges are counted. However, because of the localization of the d orbitals, the majority of the d charges have been included, except for a small portion (∼10%) that always spills out of the sphere. This leads to an error in the position of the d-band center since the point at which the d bands are half filled should no longer be exactly one-half the nominal filling. However, this error is systematic and similar in all of the compounds. On the other hand, the Bader charges of Au atoms in the various compounds are independent of the choice of the sphere.

RESULTS AND DISCUSSION

Undercoordinated Au Compounds as NP Surrogates.

As surrogates for the electronic structural features encountered in gold nanoparticles, we elected to examine the electronic structure of gold in simple periodic structures in which the Au coordination number (CN) is reduced relative to bulk *fcc*-Au, for example, simple cubic (*sc*, CN = 6) or Au-graphene (CN = 3). We begin by addressing the question of whether these hypothetical systems are valid surrogates.

Equilibrium nearest-neighbor Au−Au bond distances for *fcc*-Au and the hypothetical Au^0 structures as a function of coordination number are displayed in Figure 1. The results from first-principles calculations of Au−Au distances were taken from the published work of Paul and Narasimhan,[57] and Au−Au distances determined from molecular dynamics simulations using embedded-atom potentials, are the published results of Huang et al.[58] In order of decreasing coordination number, the structures considered include *fcc* (CN = 12), body-centered-cubic (*bcc*, CN = 8), *sc* and hexagonally close packed (*hcp*) sheet (CN = 6), diamond and square lattice (CN = 4), graphene (CN = 3), and the linear chain (CN = 2). It is particularly noteworthy that gold appears to be rather indifferent to the geometry of its surroundings: the dimensionality of the structures does not influence the preferred bond length for a given coordination number, i.e.,

dx.doi.org/10.1021/ic3002674 | Inorg. Chem. 2012, 51, 7569−7578

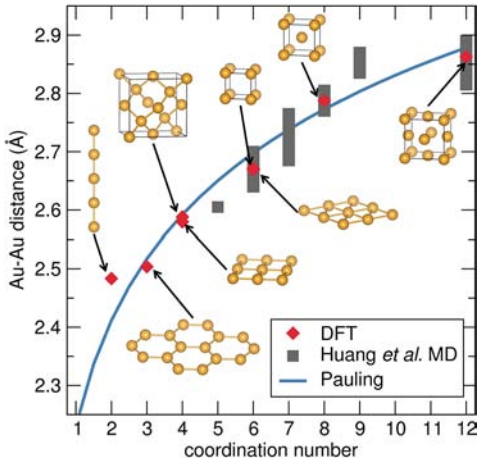

Figure 1. Equilibrium nearest-neighbor Au−Au bond length as a function of coordination number for Au in a variety of structures: *fcc* (CN = 12), *bcc* (8), *sc* and *hcp* sheet (6), diamond and square lattice (4), graphene (3), and a chain (2). DFT data is from Paul and Narasimhan,[57] and the molecular dynamics data, with embedded atom potentials, is from Huang et al.[58] The curvelabeled Pauling is an empirical bond-strength−bond-length correlation as explained in the text.

the equilibrium bond lengths are nearly identical for the *sc* lattice and *hcp* sheet and for the diamond and square lattices, respectively. These density functional predictions show remarkably close agreement with the empirical CN−bond-length relation suggested by Pauling,[59,60] as shown in eq 1

$$D_{CN} = D_{CN=1} - 0.6 \log_{10}\left(\frac{N_{VB}}{CN}\right) \quad (1)$$

where D_{CN} is the interatomic distance for a particular value of the coordination number, $D_{CN=1}$ is fixed at 2.678 Å, and the value of N_{VB}, the number of electron pairs in neutral gold, is taken to be 5.56. The validity of the relation suggests that the interatomic distance in gold structures is independent of the specifics of geometry. Additionally, the CN−bond-length relation obtained using these hypothetical Au compounds agrees well with the CN dependence found in nanoscopic gold. The structure of individual gold nanoparticles was studied using coherent electron diffraction by Huang et al.[58] Experimentally observed diffraction patterns were compared with simulated patterns generated from a coordination-number-dependent radial contraction model based on the Pauling relation and with a model obtained from molecular dynamics (MD) simulations. Coordination-number-dependent relaxation models captured some critical features of the observed patterns, and the MD model provided even better agreement. Close inspection of the MD-generated models provides great insight into the underlying complexities of surface relaxation and nanoparticle structure. Specifically, (i) coordinatively saturated atoms in the core of particles have bulk-like bond distances; strain imposed by surface relaxation propagates only ∼0.5 nm into the core. (ii) Contraction based on CN alone is insufficient to describe surface relaxation. Atoms with the same CN on different positions of the same facet display different amounts of bond-length contraction, i.e., there are strain gradients across facets. (iii) Contraction is not uniformly radial and perpendicular to the surface. On Au{100} faces, which are not close packed, the contractions are mostly parallel to the surface normal; however, atomic relaxations on the close-packed Au{111} faces have large in-plane components (perpendicular to the surface normal).[58] It is clear that a complete description of nanoparticle structure defies any traditional crystallographic model. Nonetheless, the equilibrium bond distances in the hypothetical crystallographic models that we examined, in which all of the nearest-neighbor distances are equivalent, trend very closely as a function of CN with those observed experimentally.

A similar coordination-number−bond-length correlation has been observed by Miller et al., obtained from an EXAFS study of a range of Au NP sizes.[61] We note, however, that the Au−Au distances determined in the EXAFS study are significantly longer than suggested here from the DFT calculations and also longer than those determined by Huang et al.[58] from coherent electron diffraction. The origin of the difference arises from the difficulty in accurately determining average bond lengths and coordination numbers of small nanoparticles (<5 nm), as discussed by Yevick and Frenkel.[62] When standard EXAFS fitting procedures are used to model the nongaussian distribution of bond distances in realistic NP models, average coordination numbers are underestimated and average nearest-neighbor bond distances are overestimated.

From a structural perspective, it is clear that these hypothetical compounds with reduced coordination numbers are reasonable first-approximation surrogates for undercoordinated atoms on the surface of Au nanoparticles. The next question that arises is whether the electronic structural features of these compounds are consistent with the electronic structural features of Au nanoparticles. The crucial feature suggested to impart such a dramatic change in catalytic properties in moving from the bulk state to nanoscale Au is a shift of the d-band center nearer to the Fermi energy. Such a shift occurs, for example, in the case of coordinative unsaturation (i.e., for atoms at the surface of nanoparticles)[23,24,27,63] or for a surface under tensile strain,[24] and the shift facilitates energetically favorable adsorption of molecular species.[23] In the following section, we begin to examine the Au d-state energetics of non-neutral Au compounds, during which we demonstrate that the d-band centers of the hypothetical Au compounds undergo shifts consistent with those of nanoparticulate systems.

Structures and Densities of States. The different crystal structures examined in this contribution, their space groups, and the experimental references are listed in Table 1. Structural depictions of subsets of the neutral (unary) Au, intermetallic, cationic, and anionic compounds and species investigated in the present study are shown in Figure 2. Neutral Au structures highlighted here include *fcc*, *sc*, graphene, and the linear chain.

The series of ordered intermetallics in the Ti−Au system was selected as a representative subset of intermetallic $Au^{\delta-}$ compounds with inherent structural diversity and a variety of Au environments. Ti_3Au adopts the Cr_3Si (A15) structure type, in which Au resides in the center of a Ti icosahedron. TiAu crystallizes in the CsCl structure, reducing the nearest neighbor (Au−Ti) coordination number to 8. There are no nearest-neighbor Au−Au contacts in either Ti_3Au or TiAu. There are five nearest-neighbor Au−Au contacts in $TiAu_2$ ($MoSi_2$ $C11_b$ structure), and the coordination environment can be viewed as a capped cube, compressed along the long (vertical) axis. Au caps a face comprising 4 Ti, and Ti caps a face with 4 Au. In $TiAu_4$, which has the Ni_4Mo structure, there are nine nearest-neighbor Au−Au contacts. Both Ti and Au sit at the center of

dx.doi.org/10.1021/ic3002674 | Inorg. Chem. 2012, 51, 7569−7578

Table 1. Space Groups and References to the Experimental Structures of the Au Compounds Examined in This Contribution

compound	space group	ref	compound	space group	ref
		intermetallic compounds			
Ti_3Au	$Pm\bar{3}m$	64	$TiAu_2$	$I4/mmm$	65
TiAu	$Pm\bar{3}m$	66	$TiAu_4$	$I4/m$	67
V_3Au	$Pm\bar{3}m$	68	MgAu	$Pm\bar{3}m$	69
ZnAu	$Pm\bar{3}m$	70	$BiAu_2$	$Fd\bar{3}m$	71
		cationic compounds			
AuCl	$I4_1/amd$	72	Au_2O	$Pm\bar{3}m$[a]	
AuCN	$P6mm$	73	Au_2S	$Pm\bar{3}m$	74
Au_2O_3	$Fdd2$	75	Li_5AuO_4	$Immm$[b]	76
$LaAuO_3$	$Pbcm$	77	La_4LiAuO_8	$Ammm$	78
		anionic compounds			
CsAu	$Pm\bar{3}m$	79	Cs_3AuO	$P6_3/mmc$	80
K_3AuO	$Pm\bar{3}m$	81	$BaAu_2$	$P6/mmm$	82

[a] Au_2O has not been observed experimentally but has been previously examined computationally by Shi et al.[83] [b] The crystal structure reported for Li_5AuO_4 contains site mixing between Au^{3+} and Li^+;[76] in this contribution, Li_5AuO_4 was modeled in space group *Pmmm* with Au and Li fully ordered.

cuboctahedra, with Ti surrounded by only Au, whereas three of the vertices of the cuboctahedron around Au are Ti atoms.

The Au^{3+} oxide La_4LiAuO_8 crystallizes in an ordered variant of the Nd_2CuO_4 structure containing 2D sheets with square planes of AuO_4 separated by square planes of LiO_4.[78,84] Highly electropositive La^{3+} and Li^+ countercations destabilize the O 2p states and drive strongly covalent Au−O bonding in La_4LiAuO_8, revealed by maximum entropy restoration of the electron density,[42,85] rendering the compound exceptionally stable toward thermal decomposition and reduction, particularly given the oxophobicity of gold. The Au^{1+} compounds AuCl, Au_2O, and AuCN all contain linearly coordinated gold. AuCl contains zig-zagging chains of Au and Cl; Au_2O adopts the cuprite structure, with Au forming a tetrahedron around O; and AuCN contains hexagonally close-packed sheets of Au, with the sheets separated by linear CN bridges. Among the formally Au^{1-} aurides, $BaAu_2$ can be viewed as graphene sheets of Au sandwiched between *hcp* sheets of Ba (AlB_2 structure). In the inverse-perovskite K_3AuO, Au resides on the perovskite *A* site in cuboctahedral coordination by K. Cs_3AuO adopts an inverted-$CsNiCl_3$ structure in which Au is also 12 coordinate, with 6 in-plane nearest neighbor Cs atoms plus 3 above and 3

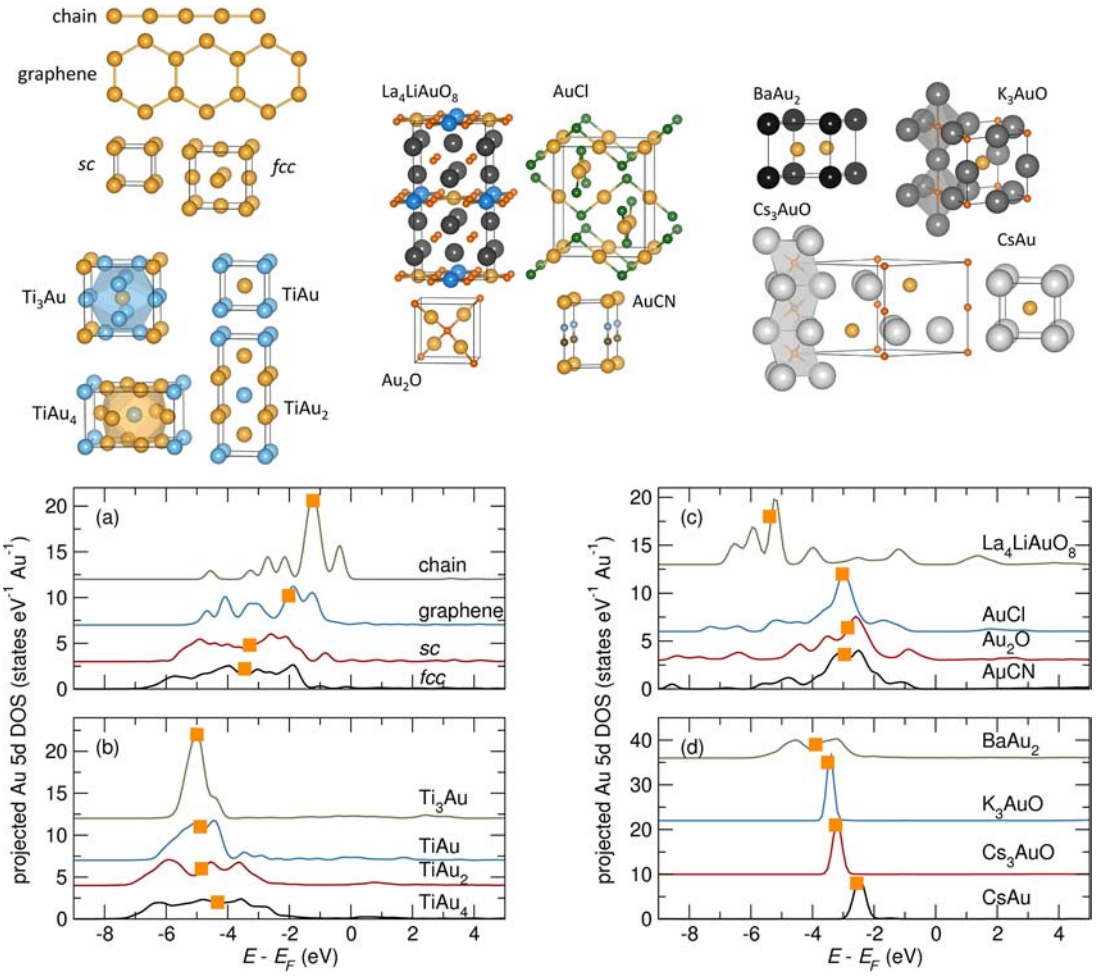

Figure 2. Structures and Au 5d-projected densities of states for a variety of compounds containing neutral, intermetallic, cationic, and anionic gold. Densities of state (DOS) of (a) neutral Au compounds, (b) ordered intermetallics in the binary Ti−Au system with structure types given in parentheses (Ti_3Au (Cr_3Si, A-15), TiAu (CsCl), $TiAu_2$ ($MoSi_2$, C11-b), and $TiAu_4$ (Ni_4Mo)), (c) compounds containing cationic Au (La_4LiAuO_8 (ordered Nd_2CuO_4), Au_2O (Cu_2O)), and (d) compounds containing the Au^{1-} auride anion: $BaAu_2$ (C32), K_3AuO (inverse perovskite), Cs_3AuO (inverse $CsNiCl_3$), CsAu (CsCl). Squares denote the position of the respective d-band centers.

dx.doi.org/10.1021/ic3002674 | *Inorg. Chem.* 2012, 51, 7569−7578

below. Perhaps the best known auride, CsAu, has the CsCl structure.

The corresponding Au 5d-projected densities of states are presented in Figure 2a for the neutral species, Figure 2b for the Ti−Au intermetallics, Figure 2c for the cationic compounds, and Figure 2d for the anionic compounds. In all cases, the DOS are normalized to a single Au atom and referenced to the Fermi energy. For semiconductors the Fermi energy is taken as the midpoint between the valence band maximum and the conduction band minimum. Squares denote the position of the Au 5d-band center.

In the neutral compounds, the d states become more localized (narrow) and the d-band center is shifted nearer to the Fermi energy as the Au coordination number is decreased in going from *fcc*-Au to a chain of atoms. The position of the d-band center is relatively insensitive to the dimensionality of a compound and shows a much more pronounced dependence on the coordination number. This is demonstrated by the four examples in Figure 3a, which shows the density of Au d states

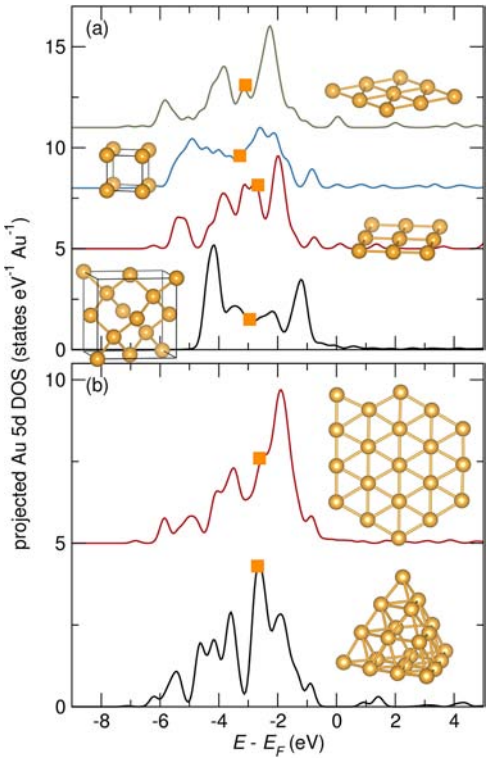

Figure 3. (a) Density of Au d states in periodic neutral gold structures with the (top to bottom) CN = 6 structures, *hcp* sheet and *sc*, and CN = 4 structures, a square lattice and diamond. For a given coordination number, the d-band center is relatively insensitive to the structural arrangement of atoms. (b) Density of Au d states in planar (top) and tetrahedral (bottom) Au_{20} clusters. Position of the d-band center is very similar for the periodic compounds and clusters, supporting the use of reduced coordination number compounds as surrogates for nanoscopic gold.

for the pairs of periodic neutral gold structures with coordination numbers of 4 and 6. The insensitivity of the d-band center to the structural arrangement supports the utility of the periodic, undercoordinated neutral Au compounds studied here as surrogates for Au nanoparticles. In Figure 3b the d-projected DOS are displayed for planar and tetrahedral clusters of Au_{20}. These clusters, which have previously been studied by some of us,[86] have d-band centers in the same region as the reduced coordination number periodic compounds, reinforcing the validity of using simple periodic structures as surrogates for nanoparticles.

The d-band center lies further from the Fermi energy in all of the Ti−Au compounds than the d center in bulk gold and is pushed increasingly lower as the amount of Ti increases. Due to the isolated nature of Au atoms in Ti_3Au and TiAu, particularly narrow band dispersions are observed. As the number of nearest-neighbor Au−Au contacts increases in going to $TiAu_2$ and $TiAu_4$, the 5d band broadens significantly. The band dispersion in $TiAu_4$ resembles that of *fcc*-Au.

Despite the overall dispersion being quite large in La_4LiAuO_8, it displays relatively localized d states, reflective of the isolation of AuO_4 units in the structure, exhibiting splitting consistent with a square planar crystal field. The experimentally determined band gap which is near 3 eV[42] is underestimated (by 2 eV), as is commonly encountered with DFT calculations. In La_4LiAuO_8, the d-band center is positioned about 5 eV below the Fermi energy. In the Au^{1+} compounds, the width and shape of the 5d states are quite similar. The d states in the anionic Au compounds in K_3AuO, Cs_3AuO, and CsAu are very narrow due to the absence of short Au−Au contacts. $BaAu_2$ is the only anionic compound in the group containing nearest-neighbor Au−Au interactions and therefore has a somewhat broader d band. However, for $BaAu_2$, the d-band center is the furthest from the Fermi energy of the aurides shown here.

We believe that the trends in the valence d states that we investigate here will not be strongly influenced by the underestimated band gaps of the insulating compounds included in this study. However, we recognize that this is dependent on the reference level for semiconducting and insulating compounds: if the Fermi energy is regarded as corresponding to the top of the valence band, then the d-band center is relatively insensitive to the magnitude of the gap because the d-band center is always below the Fermi energy. In this work, however, the Fermi energy has been referenced at the midpoint of the gap, and thus, the magnitude of the gap will shift the position of the d band downward (relative to a system referenced at the top of the valence band) by one-half the energy of the gap. Given that none of the gaps predicted are much larger than 1 eV, the position of the d band will only vary by as much as 0.5 eV, which is on the order of the scatter in the data points. It is perhaps convenient that the gaps are in some cases severely underestimated. In this regard, we are confident that the center-filling dependence is a robust one, particularly given the wide energy range over which the dependence holds. A more rigorous approach for dealing with insulating systems would be to use the vacuum level as a reference, and this is the subject of future work.

Trends in d-Band Positions in Au Compounds. Figure 4 displays the Au 5d-band center as a function of the calculated Bader charge on Au for the compounds described above and a few additional ones as well, characterized by their containing formally neutral, cationic, and anionic gold species. In addition to the *fcc*, *sc*, graphene, and chain structures that we highlighted in the previous section, the neutral Au compounds and species include *bcc*, a trimer, dimer, and an isolated Au atom, all of which were calculated in large unit cells with sufficiently large spacings between atoms employed to arrive at the appropriate structure and dimensionality.

dx.doi.org/10.1021/ic3002674 | *Inorg. Chem.* 2012, 51, 7569−7578

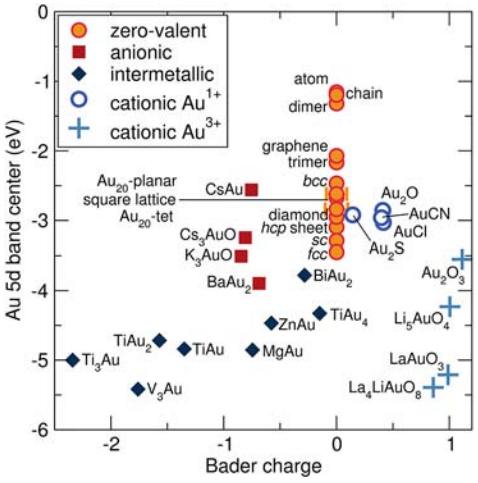

Figure 4. Position of the Au 5d-band center, relative to the Fermi energy, plotted as a function of the calculated Bader charge on Au for a wide range of gold species. There is not a strong correlation between the charge on Au, nor its formal oxidation state, and the average energy of its valence d states. Unrealistically negative Bader charges on some of the intermetallic compounds presumably arise from difficulties associated with charge density partitioning. Range of Bader charges that occur in the Au_{20} clusters are indicated with error bars.

The intermetallic compounds include those between elements with unfilled d states (Mg), partially filled d bands (Ti, V), filled d bands (Zn), and filled d with partially filled p states (Bi). In addition to the cationic gold compounds described previously, $Au_2{}^{1+}S$, $Au_2{}^{3+}O_3$, $Li_5Au^{3+}O_4$, and $LaAu^{3+}O_3$ are included in Figure 4. All of the anionic compounds that were calculated were introduced above.

We find that for the compounds calculated the Bader charges vary from zero, as expected for the neutral species, to approximately −1 for the formally anionic species such as CsAu, going to typically less than 0.5 for all the formally monovalent, cationic compounds (Au_2S, AuCN, AuCl, and Au_2O) to a maximum of a little over +1 for the formally trivalent compounds. This finding for the cationic compounds is in line with the expectation that Au is rather electronegative and the cationic compounds are therefore quite covalent. This has been specifically described earlier for trivalent La_4LiAuO_8 from both experiment and theory.[85] The intermetallic compounds studied here display Bader charges varying from −2.3 to −0.1, and the only apparent correlation is that the charges become more negative in the more Au-poor compounds.

It is clear that there is no obvious correlation between the center of the Au d states and the calculated Bader charges for the different systems examined here and indeed, between the Au d states and the formal oxidation states. What is in fact striking is that even for all the neutral species (excluding the Au_{20} clusters), although the Bader charge is zero as expected, the center of the d band tends to shift up by almost 2.5 eV toward the Fermi energy in going from 12-coordinate *fcc*-Au to a free Au atom, i.e., with decreasing coordination number. Considering the reduced coordination-number Au compounds and species as surrogates for the electronic structures of Au nanoparticles and clusters, we see that, indeed, their d-band centers are significantly closer to the Fermi energy than the d-band center of *fcc* Au, as pointed out before from calculations on Au nanoparticles[63] and clusters.[23,24,27] We additionally see that the d-band centers of most of the other systems examined here are not in this same regime of d-band center energy as undercoordinated Au. The Au_{20} clusters undergo some charge redistribution, evidenced by slightly negative Bader charges on vertex and periphery atoms. As we will later discuss, the charge redistribution in monatomic gold clusters appears to be relative to polyatomic gold compounds a special case.

The absence of any simple correlation between the position of the Au d-band center and the Bader charge is a consequence of relativistic effects which stabilize Au s states and destabilize Au d states.[87,88] Hybridization between the s, p, and d states lead to a redistribution of some d-band population into the conduction band. The degree to which gold undergoes sp−d hybridization results from the strong relativistic stabilization and contraction of the 6s (and $6p_{1/2}$) orbitals and consequent destabilization and expansion of the 5d (and 5f) orbitals.[87,88] The 6s and 5d states of gold are closer to each other in energy than the corresponding 5s/4d and 4s/3d states in Ag and Cu, and this has profound implications in the chemistry of Au, enabling a larger range of oxidation states to be accessed than in its lighter congeners. The electron affinity of gold is comparable to that of iodine,[88,89] and gold admits of halogen-like chemistry in forming (stoichiometric) ionic compounds with the alkali metals Rb and Cs.

The ready formation of Au^{1-} in compounds such as CsAu arises from Au possessing relatively stabilized s states, which also manifests as a relatively large Pauling electronegativity (for a metal) of 2.54. However, the destabilization of d states results in Au readily forming compounds in the formal +3 oxidation state (exemplified by La_4LiAuO_8). This schizophrenic behavior—summarized as s electronegative but d electropositive—is what results in the intermetallic compounds in Figure 4 displaying such a wide variation in the Au d-band center position and, indeed, sharing the same range of d-band center positions as compounds of Au that are formally 3+.

In alloys and intermetallics of gold, the strong tendency to undergo sp−d hybridization plays a crucial role in determining the average energy of the Au d band. It has been known that even in bulk gold, which has a nominally filled d shell, the d band is not occupied by an integer number of electrons.[90] Experimentally, changes in the number of unoccupied d states are readily probed with X-ray absorption spectroscopy at the transition metal *L* edge, and numerous studies have demonstrated significant modifications to occur in the occupation of the Au d band, relative to bulk gold, upon alloying. The literature is rich with XANES studies of the d-band population in random alloys and ordered intermetallics of gold with alkali,[91] main group,[92−96] and early[97,98] and late transition metals.[99−102] Despite being commonly regarded as the most electronegative transition metal, the number of unoccupied d states on Au always increases, relative to bulk gold, upon alloying. Alternative electronegativity scales, such as the one described by Watson and Bennett[103] that was derived based on the propensity of the elements to give up or receive d band electrons, are in line with this thinking.

When the center of the d states is plotted as a function of the d-band filling instead of the Bader population, as shown in Figure 5, a nearly monotonic linear dependence emerges with the center of the d band being pushed toward the Fermi energy as the 5d filling increases. The d filling was calculated as explained in the Methods section. We note that the values for the filling should not be regarded as actual electron counts, since the band integration procedure systematically omits some

dx.doi.org/10.1021/ic3002674 | *Inorg. Chem.* 2012, 51, 7569−7578

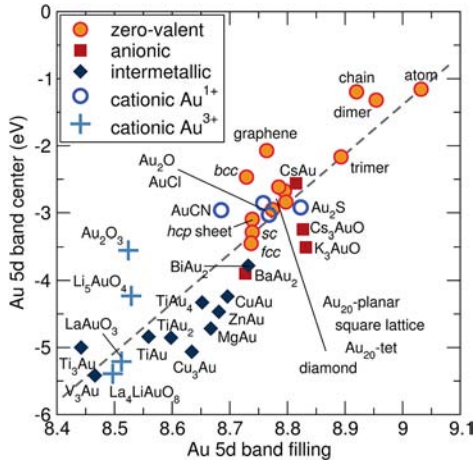

Figure 5. Position of the Au 5d-band center, relative to the Fermi energy, plotted as a function of the Au 5d-band population. Despite rather modest changes in the degree of filling, <0.6 *e* difference between Ti_3Au and a free Au atom, the effect on the average energy of the d states is surprisingly large. Dotted gray line is a linear regression and shown to guide the eye.

of the electron population. However, as this omitted population is comparable across the different compounds, the trends reported here should be robust. The scatter of the data points arises from additional factors that influence the position of the d-band center, and in this regard it is important to point out that our intention is not to suggest that the d-band filling is the only determinant of the energy of the Au d states. However, it is quite clear that the d-band filling is strongly correlated with the position of the d-band center across the wide range of chemical environments probed here. This is particularly notable given the widely varying position and width of the d band in the many compounds studied here; in this regard, the strong dependence between the d-band center and d-band filling is not a trivial relationship. Indeed, for two equal-shaped and rigid bands with distinct electron filling, the center of the band should actually be lower in the system with higher filling, and the trend observed here is precisely the converse.

In the study of late transition metal surfaces it is commonly approximated that the filling of the d band remains constant for a given metal upon alloying with other transition metals.[32,33,104−106] This is often a reasonable assumption, as calculated changes in absolute charge are typically on the order of 0.1 *e* for many alloys, consistent with the restrictions of electroneutrality. Assuming constant band filling enables changes in the d-band centroid to be readily evaluated within the context of a rectangular band model. In such a picture, because the d electrons are "pinned" at the Fermi energy changes in the position of the centroid can be interpreted as resulting from alterations in the dispersion of the d band. For the situation of a band that is more than half filled, band broadening that would occur because of an increase in coordination number or orbital overlap would result in a lowering of the d-band center. Reducing the coordination number would lead to a narrowing of the d states, pushing the centroid closer to the Fermi energy. As it pertains to the gold compounds studied here, a constant filling model guided by differences in bandwidth cannot be used to reconcile variations in the Au 5d-band center. One such example is the Ti−Au series shown in Figure 2b, where it is seen that the d-band center moves away from the Fermi energy as the Au 5d bandwidth decreases.

Of all the compounds and species shown in Figure 5, Au_2O_3 stands out as an outlier, which may due to difficulty in accurately describing its electronic structure using the methods employed here. Comparing K_3AuO, Cs_3AuO, and CsAu, there are only small changes in the d-band filling but possibly significant differences in the position of the d-band center. The centroid of CsAu lies about 1 eV closer to the Fermi level than that of K_3AuO and about 0.75 eV closer to E_F than the d-band center in Cs_3AuO. The difference can be understood in terms of the increasing interaction between Au and the highly electropositive K and Cs cations that is screened by the oxide anion and is strongest in CsAu. As a cautionary note in interpreting the trend of the d-band position in these three compounds, the valence bands in K_3AuO and Cs_3AuO derive mostly from O p states, unlike the case of CsAu, where the valence band is purely Au derived. This difference can result in differing reference Fermi energies that would influence the trend.

In the case of gold nanoparticles, Coulthard et al. found that Au NPs supported on porous silica displayed a decreased XANES white-line intensity, relative to bulk gold, indicating a greater filling of the Au d states.[107] More recently, Miller and van Bokhoven reported an extensive L_3 edge XANES and EXAFS study of Au NPs ranging in size from about 1 to 5 nm and deposited on a variety of different supports.[27] They showed that the filling of the Au d band as interpreted from XANES white-line intensity increases in smaller particles and that the d-band population is independent of the support on which the particles are dispersed. This finding was further borne out in the same study by quantum chemical calculations for Au clusters, which indicated a greater degree of filling in the Au d band and a concurrent shift of the d-band centroid toward the Fermi energy for smaller particles and for surface atoms relative to coordinatively saturated atoms. Enrichment of the d-band population in undercoordinated atoms is consistent with Au 4f XPS studies of the surface contribution in bulk gold, which was found to shift to lower binding energy relative to the bulk value.[108]

In fact, almost all Au-based bimetallic nanoparticulate catalysts are alloys of Au with other late transition metals, which do not drain the Au 5d filling to the extent that early transition metals such as Ti do. For example, it is known for bulk and nano PtAu alloys the Au d band is slightly depopulated relative to bulk Au. However, in nanoparticles, this depopulation of states can potentially be compensated by reduction of the coordination number (band narrowing) and increased covalency due to shorter distances between atoms.[109] Given the importance of the d-band population, the charge redistribution that occurs in bimetallic nanoparticles is not necessarily well probed by analyses such as the Bader or Mulliken methods. Although we observe an increase in both the Bader chages and d-band filling for atoms at the periphery or vertices of the Au_{20} clusters relative to atoms with higher coordination numbers, this may be a special case limited to monometallic Au. In bimetallic nanoparticles of Au there is a balance between depopulation and redistribution of the d-band charge due to alloying and increasing population of the d band due to reducing the coordination number, which potentially will not be captured in population analyses that consider the entire atomic charge.

dx.doi.org/10.1021/ic3002674 | *Inorg. Chem.* 2012, 51, 7569−7578

We attribute the strong d center−charge dependence to arise from Coulomb repulsion of d electrons. Because of the increased electron repulsion, greater filling destabilizes the d states, pushing the d-band center nearer to the Fermi energy. In order to understand the cause of the strong center−charge dependence and to examine the applicability to other transition metals, we calculated the d-band center and d-band filling for compounds and species of Ag. As shown in Figure 6, Ag

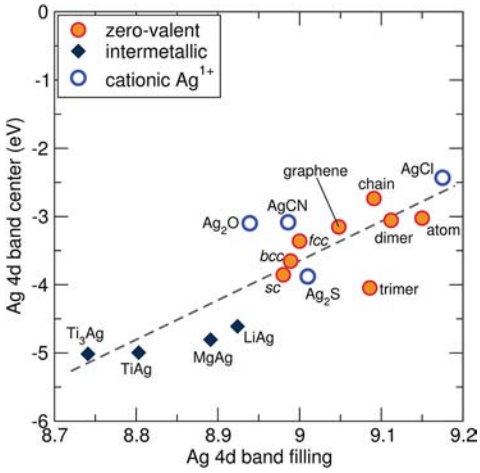

Figure 6. Position of the Ag 4d-band center, relative to the Fermi energy, as a function of the Ag 4d-band population for a variety of neutral, intermetallic, and cationic Ag compounds and species.

compounds show a similar dependence for the d-band center and filling. However, the slope is smaller than for the Au compounds, i.e., the Ag 4d-band center does not change as dramatically as a function of the d-band filling relative to Au. One suggestion for the weaker dependence of the d-band center on the d-band population for the Ag compounds is that the d bands in Ag compounds are stabilized in contrast to the d bands in Au compounds which are subject to relativistic destabilization.[87,88] It is evident from a consideration of the d-band centers of the gold compounds and species in Figure 5 with the d-band centers of the Ag compounds and species in Figure 6 that only for the Au case is the d band found within −1 and −3 eV of the Fermi energy. This supports the finding that Ag compounds and species, including nanoparticles, are not commonly used as CO oxidation catalysts.

The electron−electron interaction is only treated in a mean-field fashion in DFT-GGA calculations. Since we suggested that the strong d-center−d-filling dependence is likely Coulombic in origin, it is germane to consider how robust this dependence is when Coulomb correlations are included more explicitly via the Hubbard *U*. As shown in Figure 7, Au shows a strong d-center−d-filling dependence with a Hubbard *U* of 3 eV. The trend for Au is very similar to that obtained without a Hubbard *U*, except for a downward shift of the band centers and increased d-band filling caused by *U*.

CONCLUSIONS

First-principles electronic structure calculations carried out on a variety of Au compounds and species suggest the complete (and surprising) absence of any correlation between the position of the Au d-band center and the formal oxidation state or Bader charge on Au. The results additionally suggest that very few Au compounds have d-band centers in the region

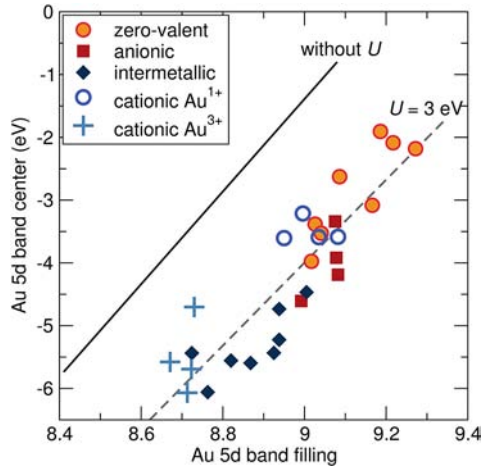

Figure 7. Au 5d-band center, relative to the Fermi energy, plotted as a function of the Au 5d-band population, calculated using a Hubbard *U* = 3 eV. Fit (dashed line) to data calculated without a *U* term is shown for comparison. Introducing *U* shifts the d-band center away from the Fermi energy and increases the calculated filling of the 5d band.

of energy that seem to be implicated in the catalytic activity of Au nanoparticles. We find strong dependence between the position of the Au d-band center and the degree of its filling, irrespective of the chemistry or the geometry of the particular Au compound. Even small calculated changes in the d-band filling result in a relatively large effect on the position of the d-band center.

AUTHOR INFORMATION

Corresponding Author

*E-mail: seshadri@mrl.ucsb.edu.

Notes

The authors declare no competing financial interest.

ACKNOWLEDGMENTS

It is a pleasure to thank Horia Metiu and Karin Rabe for sharing their insights and Karin Rabe for critically reading this manuscript. We also thank Dane Morgan for sharing a key preprint. We thank the Department of Energy, Office of Basic Energy Sciences, for support of this work through DE-FG02-10ER16081. This work made use of the computing facilities of the Center for Scientific Computing supported by the California Nanosystems Institute, Hewlett-Packard, and by the Materials Research Laboratory at UCSB: an NSF MRSEC (DMR-1121053).

REFERENCES

(1) Dulong, P.-L.; Thenard, L.-G. *Ann. Chim. Phys.* **1823**, *24*, 380.
(2) Dulong, P.-L.; Thenard, L.-G. *Ann. Chim. Phys.* **1823**, *23*, 440.
(3) Haruta, M.; Kobayashi, T.; Sano, H.; Yamada, N. *Chem. Lett.* **1987**, *2*, 405−408.
(4) Valden, M.; Lai, X.; Goodman, D. *Science* **1998**, *281*, 1647−1650.
(5) Yang, Z.; Wu, R.; Goodman, D. *Phys. Rev. B* **2000**, *61*, 14066−14071.
(6) Grunwaldt, J.-D.; Baiker, A. *J. Phys. Chem. B* **1999**, *103*, 1002−1012.
(7) Guzman, J.; Gates, B. *J. Phys. Chem. B* **2002**, *106*, 7659−7665.
(8) Costello, C.; Guzman, J.; Yang, J.; Wang, Y.; Kung, M.; Gates, B.; Kung, H. *J. Phys. Chem. B* **2004**, *108*, 12529−12536.
(9) Fierro-Gonzalez, J.; Gates, B. *J. Phys. Chem. B* **2004**, *108*, 16999−17002.

(10) Schwartz, V.; Mullins, D.; Yan, W.; Chen, B.; Dai, S.; Overbury, S. *J. Phys. Chem. B* **2004**, *108*, 15782−15790.
(11) Zanella, R.; Giorgio, S.; Shin, C.; Henry, C.; Louis, C. *J. Catal.* **2004**, *222*, 357−367.
(12) Yang, J. H.; Henao, J. D.; Raphulu, M. C.; Wang, Y. M.; Caputo, T.; Groszek, A. J.; Kung, M. C.; Scurrell, M. S.; Miller, J. T.; Kung, H. H. *J. Phys. Chem. B* **2005**, *109*, 10319−10326.
(13) Hutchings, G. J.; Hall, M. S.; Carley, A. F.; Landon, P.; Solsona, B. E.; Kiely, C. J.; Herzing, A.; Makkee, M.; Moulijn, J. A.; Overweg, A.; Fierro-Gonzalez, J. C.; Guzman, J.; Gates, B. C. *J. Catal.* **2006**, *242*, 71−81.
(14) Weiher, N.; Bus, E.; Delannoy, L.; Louis, C.; Ramaker, D.; Miller, J.; van Bokhoven, J. *J. Catal.* **2006**, *240*, 100−107.
(15) Weiher, N.; Beesley, A. M.; Tsapatsaris, N.; Delannoy, L.; Louis, C.; van Bokhoven, J. A.; Schroeder, S. L. M. *J. Am. Chem. Soc.* **2007**, *129*, 2240−2241.
(16) Fierro-Gonzalez, J. C.; Guzman, J.; Gates, B. C. *Top. Catal.* **2007**, *44*, 103−114.
(17) Fu, Q.; Saltsburg, H.; Flytzani-Stephanopoulos, M. *Science* **2003**, *301*, 935−938.
(18) Fu, Q.; Deng, W. L.; Saltsburg, H.; Flytzani-Stephanopoulos, M. *Appl. Catal. B: Environ.* **2005**, *56*, 57−68.
(19) Liu, Z. P.; Jenkins, S. J.; King, D. A. *Phys. Rev. Lett.* **2005**, *94*, 196102−1−4.
(20) Tibiletti, D.; Amieiro-Fonseca, A.; Burch, R.; Chen, Y.; Fisher, J. M.; Goguet, A.; Hardacre, C.; Hu, P.; Thompsett, A. *J. Phys. Chem. B* **2005**, *109*, 22553−22559.
(21) Williams, W. D.; Shekhar, M.; Lee, W.-S.; Kispersky, V.; Delgass, W. N.; Ribeiro, F. H.; Kim, S. M.; Stach, E. A.; Miller, J. T.; Allard, L. F. *J. Am. Chem. Soc.* **2010**, *132*, 14018−14020.
(22) Mavrikakis, M.; Stoltze, P.; Nørskov, J. *Catal. Lett.* **2000**, *64*, 101−106.
(23) Lopez, N.; Nørskov, J. *J. Am. Chem. Soc.* **2002**, *124*, 11262−11263.
(24) Lopez, N.; Janssens, T.; Clausen, B.; Xu, Y.; Mavrikakis, M.; Bligaard, T.; Nørskov, J. *J. Catal.* **2004**, *223*, 232−235.
(25) Overbury, S. H.; Schwartz, V.; Mullim, D. R.; Yan, W.; Dai, S. *J. Catal.* **2006**, *241*, 56−65.
(26) Janssens, T. V. W.; Clausen, B. S.; Hvolbaek, B.; Falsig, H.; Christensen, C. H.; Bligaard, T.; Nørskov, J. K. *Top. Catal.* **2007**, *44*, 15−26.
(27) van Bokhoven, J. A.; Miller, J. T. *J. Phys. Chem. C* **2007**, *111*, 9245−9249.
(28) Taylor, H. S. *Proc. R. Soc. London Ser. A* **1925**, *108*, 105−111.
(29) Xu, C.; Xu, X.; Su, J.; Ding, Y. *J. Catal.* **2007**, *252*, 243−248.
(30) Hammer, B.; Nørskov, J. K. *Nature* **1995**, *376*, 238−240.
(31) Hammer, B.; Nørskov, J. K. *Surf. Sci.* **1995**, *343*, 211−220.
(32) Ruban, A.; Hammer, B.; Stoltze, P.; Skriver, H.; Nørskov, J. *J. Mol. Cat. A* **1997**, *115*, 421−429.
(33) Pedersen, M.; Helveg, S.; Ruban, A.; Stensgaard, I.; Laegsgaard, E.; Nørskov, J.; Besenbacher, F. *Surf. Sci.* **1999**, *426*, 395−409.
(34) Nørskov, J. K.; Bligaard, T.; Rossmeisl, J.; Christensen, C. H. *Nature Chem.* **2009**, *1*, 37−46.
(35) Nørskov, J. K.; Abild-Pedersen, F.; Studt, F.; Bligaard, T. *Proc. Natl. Acad. Sci. U.S.A.* **2011**, *108*, 937−943.
(36) Nørskov, J.; Bligaard, T.; Logadottir, A.; Bahn, S.; Hansen, L.; Bollinger, M.; Bengaard, H.; Hammer, B.; Sljivancanin, Z.; Mavrikakis, M.; Xu, Y.; Dahl, S.; Jacobsen, C. *J. Catal.* **2002**, *209*, 275−278.
(37) Jacobsen, C.; Dahl, S.; Clausen, B.; Bahn, S.; Logadottir, A.; Nørskov, J. *J. Am. Chem. Soc.* **2001**, *123*, 8404−8405.
(38) Stamenkovic, V.; Mun, B.; Mayrhofer, K.; Ross, P.; Markovic, N.; Rossmeisl, J.; Greeley, J.; Nørskov, J. *Angew. Chem., Int. Ed.* **2006**, *45*, 2897−2901.
(39) Studt, F.; Abild-Pedersen, F.; Bligaard, T.; Sørensen, R. Z.; Christensen, C. H.; Nørskov, J. K. *Science* **2008**, *320*, 1320−1322.
(40) Chretien, S.; Gordon, M. S.; Metiu, H. *J. Chem. Phys.* **2004**, *121*, 3756−3766.
(41) Chretien, S.; Buratto, S. K.; Metiu, H. *Curr. Opin. Solid State Mater. Sci.* **2007**, *11*, 62−75.
(42) Kurzman, J. A.; Ouyang, X.; Im, W. B.; Li, J.; Hu, J.; Scott, S. L.; Seshadri, R. *Inorg. Chem.* **2010**, *49*, 4670−4680.
(43) Hegde, M. S.; Madras, G.; Patil, K. C. *Acc. Chem. Res.* **2009**, *42*, 704−712.
(44) Jansen, M. *Chem. Soc. Rev.* **2008**, *37*, 1824−1835.
(45) Rodriguez, J. A.; Hrbek, J.; Kuhn, M.; Sham, T. K. *J. Phys. Chem.* **1993**, *97*, 4737−4744.
(46) Carley, A. F.; Roberts, M. W.; Santra, A. K. *J. Phys. Chem. B* **1997**, *101*, 9978−9983.
(47) Kresse, G.; Hafner, J. *Phys. Rev. B* **1993**, *47*, 558−561.
(48) Kresse, G.; Furthmüller, J. *Phys. Rev. B* **1996**, *54*, 11169.
(49) Blöchl, P. E. *Phys. Rev. B* **1994**, 17953.
(50) Kresse, G.; Joubert, D. *Phys. Rev. B* **1999**, *59*, 1758−1775.
(51) Perdew, J. P.; Burke, K.; Ernzerhof, M. *Phys. Rev. Lett.* **1996**, *77*, 3865.
(52) Bergerhoff, G.; Brown, I. D. *Crystallogr. Databases* **1987**, AUTHOR: PLEASEPROVIDE VOLUME, PAGE NUMBER(S), or DOI.
(53) Nautiyal, T.; Youn, S. J.; Kim, K. S. *Phys. Rev. B* **2003**, *68*, 033407:1−4.
(54) Yang, X.; Zhou, J.; Weng, H.; Dong, J. *Appl. Phys. Lett.* **2008**, *92023115*.
(55) Henkelman, G.; Arnaldsson, A.; Jónsson, H. *Comput. Mater. Sci.* **2006**, *34*, 354−360.
(56) Bader, R. F. W. *Atoms in Molecules: A Quantum Theory*; Oxford: Oxford University Press: Oxford, UK, 1990.
(57) Paul, J.; Narasimhan, S. *Bull. Mater. Sci.* **2008**, *31*, 569−572.
(58) Huang, W. J.; Sun, R.; Tao, J.; Menard, L. D.; Nuzzo, R. G.; Zuo, J. M. *Nat. Mater.* **2008**, *7*, 308−313.
(59) Pauling, L. *The Nature of the Chemical Bond*, 3rd ed.; Cornell University Press: Ithaca, NY, 1960.
(60) Pauling, L. *J. Am. Chem. Soc.* **1947**, *69*, 542−533.
(61) Miller, J. T.; Kropf, A. J.; Zha, Y.; Regalbuto, J. R.; Delannoy, L.; Louis, C.; Bus, E.; van Bokhoven, J. A. *J. Catal.* **2006**, *240*, 222−234.
(62) Yevick, A.; Frenkel, A. I. *Phys. Rev. B* **2010**, *81*, 115451.
(63) Zhang, X.; Kuo, J.-L.; Gu, M.; Fan, X.; Bai, P.; Song, Q.-G.; Sun, C. Q. *Nanoscale* **2010**, *2*, 412−417.
(64) Vonphilipshorn, H.; Laves, F. *Acta Crystallogr.* **1964**, *17*, 213.
(65) Schubert, K.; Balk, M.; Bhan, S.; Breimer, H.; Esslinger, P.; Stolz, E. *Naturwissenschaften* **1959**, *46*, 647−648.
(66) Donkersl, H. C.; Vanvucht, J. H. *J. Less Common Metals* **1970**, *20*, 83.
(67) Pietrokowsky, P. *J. Inst. Met.* **1962**, *90*, 434.
(68) Wood, E. A.; Matthias, B. T. *Acta Crystallogr.* **1956**, *9*, 534.
(69) Brauer, G.; Haucke, W. *Z. Phys. Chem. B: Chem. E* **1936**, *33*, 304−310.
(70) Owen, E. A.; Preston, G. D. *Philos. Mag. Ser. 7* **1926**, *2*, 1266−1270.
(71) Jurriaanse, T. *Z. Kristallogr., Kristallgeom., Kristallphys., Kristallchem.* **1935**, *90*, 322−329.
(72) Janssen, E. M. W.; Folmer, J. C. W.; Wiegers, G. A. *J. Less Common Met.* **1974**, *38*, 71−76.
(73) Bowmaker, G. A.; Kennedy, B. J.; Reid, J. C. *Inorg. Chem.* **1998**, *37*, 3968−3974.
(74) Hirsch, H.; Decugnac, A.; Gadet, M. C.; Pouradie, J. *C. R. Acad. Sci. B Phys.* **1966**, *263*, 1328.
(75) Jones, P. G.; Rumpel, H.; Schwarzmann, E.; Sheldrick, G. M.; Paulus, H. *Acta Crystallogr. B* **1979**, *35*, 1435−1437.
(76) Waselnie, H. D.; Hoppe, R. *Z. Anorg. Allg. Chem.* **1970**, *375*, 43.
(77) Ralle, M.; Jansen, M. *J. Solid State Chem.* **1993**, *105*, 378−384.
(78) Pietzuch, W.; Warda, S. A.; Massa, W.; Reinen, D. *Z. Anorg. Allg. Chem.* **2000**, *626*, 113−117.
(79) Kienast, G.; Verma, J.; Klemm, W. *Z. Anorg. Allg. Chem.* **1961**, *310*, 143−169.
(80) Feldmann, C.; Jansen, M. *Angew. Chem., Int. Ed.* **1993**, *32*, 1049−1050.
(81) Feldmann, C.; Jansen, M. *Z. Anorg. Allg. Chem.* **1995**, *621*, 201−206.
(82) Bruzzone, G. *Atti. Accad. Naz. Lin.* **1970**, *48*, 235−241.

(83) Shi, H.; Asahi, R.; Stampfl, C. *Phys. Rev. B* **2007**, *75*, 205125.
(84) Abbattista, F.; Vallino, M.; Mazza, D. *J. Less-Common Met.* **1985**, *110*, 391−396.
(85) Kurzman, J. A.; Moffitt, S. L.; Llobet, A.; Seshadri, R. *J. Solid State Chem.* **2011**, *184*, 1439−1444.
(86) Mammen, N.; Narasimhan, S.; de Gironcoli, S. *J. Am. Chem. Soc.* **2011**, *133*, 2801−2803.
(87) Pitzer, K. S. *Acc. Chem. Res.* **1979**, *12*, 271−276.
(88) Pyykkoö, P.; Desclaux, J. *Acc. Chem. Res.* **1979**, *12*, 276−281.
(89) Jansen, M. *Solid State Sci.* **2005**, *7*, 1464−1474.
(90) Mason, M. *Phys. Rev. B* **1983**, *27*, 748−762.
(91) Watson, R.; Weinert, M. *Phys. Rev. B* **1994**, *49*, 7148−7154.
(92) Friedman, R.; Hudis, J.; Perlman, M.; Watson, R. *Phys. Rev. B* **1973**, *8*, 2433−2440.
(93) Sham, T.; Perlman, M.; Watson, R. *Phys. Rev. B* **1979**, *19*, 539−545.
(94) Jeon, Y.; Qi, B.; Lu, F.; Croft, M. *Phys. Rev. B* **1989**, *40*, 1538−1545.
(95) Bzowski, A.; Yiu, Y.; Sham, T. *Phys. Rev. B* **1995**, *51*, 9515−9520.
(96) Palade, P.; Wagner, F.; Jianu, A.; Filoti, G. *J. Alloys Compd.* **2003**, *353*, 23−32.
(97) Bzowski, A.; Sham, T. *J. Vac. Sci. Technol. A* **1993**, *11*, 2153−2157.
(98) Naftel, S.; Bzowski, A.; Sham, T. *J. Alloys Compd.* **1999**, *283*, 5−11.
(99) Chou, T.; Perlman, M.; Watson, R. *Phys. Rev. B* **1976**, *14*, 3248−3250.
(100) Sham, T.; Yiu, Y.; Kuhn, M.; Tan, K. *Phys. Rev. B* **1990**, *41*, 11881−11886.
(101) Tyson, C.; Bzowski, A.; Kristof, P.; Kuhn, M.; Sammynaiken, R.; Sham, T. *Phys. Rev. B* **1992**, *45*, 8924−8928.
(102) Kuhn, M.; Bzowski, A.; Sham, T. *Hyperfine Interact.* **1994**, *94*, 2267−2272.
(103) Watson, R.; Bennett, L. *Phys. Rev. B* **1978**, *18*, 6439−6449.
(104) Mavrikakis, M.; Hammer, B.; Nørskov, J. K. *Phys. Rev. Lett.* **1998**, *81*, 2819−2822.
(105) Kitchin, J.; Nørskov, J.; Barteau, M.; Chen, J. *Phys. Rev. Lett.* **2004**, *93*, 156801.
(106) Kitchin, J.; Nørskov, J.; Barteau, M.; Chen, J. *J. Chem. Phys.* **2004**, *120*, 10240−10246.
(107) Coulthard, I.; Degen, S.; Zhu, Y.; Sham, T. *Can. J. Chem.* **1998**, *76*, 1707−1716.
(108) Citrin, P.; Wertheim, G.; Baer, Y. *Phys. Rev. Lett.* **1978**, *41*, 1425−1428.
(109) Bus, E.; van Bokhoven, J. A. *J. Phys. Chem. C* **2007**, *111*, 9761−9768.